PROCEEDINGS A

royalsocietypublishing.org/journal/rspa

Research



Cite this article: Heo H, Walker E, Zubov Y, Shymkiv D, Wages D, Krokhin A, Choi T-Y, Neogi A. 2020 Non-reciprocal acoustics in a viscous environment. *Proc. R. Soc. A* **476**: 20200657. https://doi.org/10.1098/rspa.2020.0657

Received: 15 August 2020 Accepted: 11 November 2020

Subject Areas:

acoustics

Keywords:

non-reciprocity, rough surface scattering, viscous losses

Author for correspondence:

Arkadii Krokhin

e-mail: arkady@unt.edu

Non-reciprocal acoustics in a viscous environment

Hyeonu Heo¹, Ezekiel Walker², Yurii Zubov¹, Dmitrii Shymkiv¹, Dylan Wages³, Arkadii Krokhin¹, Tae-Youl Choi³ and Arup Neogi¹

¹Department of Physics, University of North Texas, PO Box 311427, Denton, TX 76203, USA

²Echonovus Inc., 1800 South Loop 288 STE 396 #234, Denton, TX 76205, USA

³Department of Mechanical Engineering, University of North Texas, 3940 North Elm Suite F101, Denton, TX 76207, USA

AK, 0000-0002-8910-5241

It is demonstrated that acoustic transmission through a phononic crystal with anisotropic solid scatterers becomes non-reciprocal if the background fluid is viscous. In an ideal (inviscid) fluid, the transmission along the direction of broken P symmetry is asymmetric. This asymmetry is compatible with reciprocity since time-reversal symmetry (T symmetry) holds. Viscous losses break T symmetry, adding a non-reciprocal contribution to the transmission coefficient. The non-reciprocal transmission spectra for a phononic crystal of metallic circular cylinders in water are experimentally obtained and analysed. The surfaces of the cylinders were specially processed in order to weakly break P symmetry and increase viscous losses through manipulation of surface features. Subsequently, the non-reciprocal part of transmission is separated from its asymmetric reciprocal part in numerically simulated transmission spectra. The level of nonreciprocity is in agreement with the measure of broken P symmetry. The reported study contradicts commonly accepted opinion that linear dissipation cannot be a reason leading to non-reciprocity. It also opens a way for engineering passive acoustic diodes exploring the natural viscosity of any fluid as a factor leading to non-reciprocity.

1. Introduction

Distribution of acoustic pressure $p_A(\mathbf{r})$ produced by a point source at position \mathbf{r}_A in an inhomogeneous fluid

with arbitrary distribution of scatterers satisfies a reciprocity relation formulated in its simplest form by Rayleigh [1]

$$p_A(\mathbf{r}_B) = p_B(\mathbf{r}_A). \tag{1.1}$$

This relation expresses a symmetry between emitter and receiver upon switching their positions. More general reciprocity relations valid for distributed sources, such as anisotropic, moving and porous media and transient signals have been reported, expressed in the form of convolution or correlation integrals [2–12]. One more important characteristic of acoustic fields is the vector of the local velocity of an oscillating fluid. In an ideal fluid (inviscid), this vector is related to the gradient of pressure, $\mathbf{v}(\mathbf{r}) = \nabla p/i\omega\rho$, where $\rho(\mathbf{r})$ is the fluid density and $\omega/2\pi$ is the frequency of the monochromatic source. As a whole, $\mathbf{v}(\mathbf{r})$ is not a reciprocal vector. Only its projections in certain directions turn out to be reciprocal. For example, for a dipole source (with moment along direction \mathbf{n}) emitting in ideal fluid, the reciprocal theorem for velocity takes the form [13]:

$$\rho_A \mathbf{v}_B(\mathbf{r}_A) \cdot \mathbf{n}_A = \rho_B \mathbf{v}_A(\mathbf{r}_B) \cdot \mathbf{n}_B. \tag{1.2}$$

Even in a homogeneous fluid, $\rho_A = \rho_B$, the projections of vector $\mathbf{v}(\mathbf{r})$ in directions different from \mathbf{n} remain non-reciprocal. In ideal fluids, pressure plays the role of the scalar potential for velocity, $\mathbf{v} \sim \nabla p$. The Rayleigh reciprocity theorem [1] is formulated for velocity potentials but not for their gradients. Any function of the absolute value of velocity, $v(\mathbf{r})$, turns out to be non-reciprocal. In particular, a condition similar to equation (1.1) is not valid for acoustic intensity I = pv.

For a system with anisotropic scatterers, the lack of reciprocal symmetry leads to asymmetry of the transmission coefficient. This property has been used for the design of sound rectification devices [14–21]. While they provide almost unidirectional propagation of sound, they are considered to be reciprocal by nature [22] since they do not break time-reversibility, if dissipative losses are neglected.

Dissipation is a natural cause of increasing entropy that makes propagation of sound irreversible. However, there is a common belief that transmission of sound remains reciprocal even in a dissipative medium, e.g. the recent reviews [22–24]. Dissipation can be phenomenologically introduced by adding imaginary parts to elastic moduli. Apparently, this does not change the dynamical equations for sound waves, which remain reciprocal [6,7]. The dynamics of a viscous fluid is given by the Navier-Stokes equation, which is not time-reversible. Microscopic calculations of viscous losses require solutions of the Navier-Stokes equation for the field of velocities $\mathbf{v}(\mathbf{r})$. In general, this field is not symmetric with respect to switching the positions of emitter and receiver. Due to asymmetry of the field of velocities, the local dissipation of acoustic energy defined through gradients of velocity, $\partial v_i/\partial x_k$, is also asymmetrical, i.e. the amount of dissipated energy is different for opposing directions of propagation. Accordingly, the transmission coefficient, which is already asymmetrical in ideal fluids, acquires an additional dissipative part in viscous fluid. This part is truly non-reciprocal because it is due to the viscous mechanism that breaks time reversibility. The main goal of this study is to demonstrate that linear viscous dissipation in fluids is a factor that breaks non-reciprocity in transmission and that these two contributions—asymmetric and non-reciprocal—can be discriminated.

Of course, viscous dissipation affects transmission of any phononic crystals, including twodimensional samples of circular cylinders. While the *T* symmetry in those samples is broken by viscous losses, the transmission remains reciprocal along any direction. A necessary condition for non-reciprocal transmission is broken *P* symmetry of the scatterers. Thus, linear dissipation leads to non-reciprocal transmission if *PT* symmetry is broken. Non-reciprocal transmission of elastic and acoustic waves through a phononic crystal of asymmetric rods caused by viscous losses was reported in [25,26].

A case of one-dimensional systems requires special attention. Since the vector \mathbf{v} has a single component, its reciprocity in ideal fluid follows from equation (1.2). Reciprocity of projection of velocity in a viscous fluid was mentioned in a short note [27]. Then, the intensity I=pv is also reciprocal even for asymmetric distribution of scatterers. The transmission coefficient is independent of direction of the incoming wave and asymmetry is manifested through different reflection coefficients for the waves coming from the left and right, $r_L \neq r_R$. In the presence of

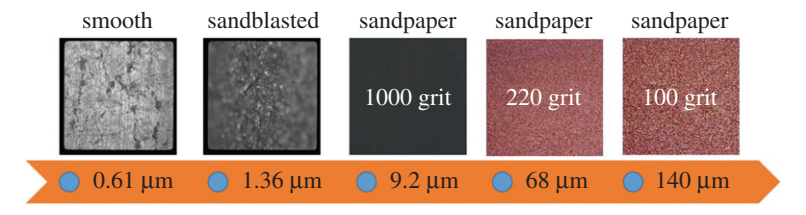


Figure 1. The average height of surface roughness ranging from 0.61 μ m (\sim 10⁻⁴ λ) to 140 μ m (\sim 10⁻¹ λ). Five different levels of roughness that weakly break *P* symmetry are examined. The surface of bare stainless steel rods is approximated as flat. (Online version in colour.)

energy losses, the left and right absorption coefficient may differ essentially, while transmission remains reciprocal [21,28–32].

We present here experimental and numerical evidence that acoustic transmission through a two-dimensional phononic crystal with broken *PT* symmetry contains two contributions: asymmetrical and non-reciprocal. In order to emphasize the non-reciprocal part, the geometry of the scatterers is chosen to be such that the effects of asymmetry are minimized. The scatterers are rods of circular cross section. One half of the cylindrical surface is smooth and the other half is rough. Asymmetry, due to scattering at the rough surface, is small since the wavelength is much greater than the size of the roughness. On the other hand, the viscous energy losses near a rough surface are strongly enhanced if the size of the roughness exceeds the thickness of the viscous boundary layer [33]. It is important to note that the non-reciprocal part exists only due to asymmetry in the surface features of the otherwise symmetric cylinder. If the scatterers are *P* symmetric the viscous losses in transmission become independent of the direction of propagation, while transmission remains irreversible.

Difference in transmission serves as a signature of reciprocity/non-reciprocity for finite-size samples. In an infinite phononic crystal, propagating wave is characterized by dispersion relation $\omega(\mathbf{k})$. Here, we give an analytical proof that in an infinite phononic crystal with broken PT symmetry, the dispersion relation remains reciprocal, while the distribution of velocities loses the symmetry that provides reciprocity in a dissipationless phononic crystal. Thus, although the dispersion relation remains reciprocal, the eigenfunctions become non-reciprocal, which has strong impacts for finite samples.

2. Experimental set-up and transmission spectra

To minimize the asymmetric part of transmission, cylindrical stainless steel rods with various sizes of surface roughness were used (figure 1) as scatterers for two-dimensional phononic crystal (figure 2). Each rod is half-covered by roughness of different type and size. Controlled roughness was introduced to the rods using sandblasting and sandpaper of varying grain sizes where the average roughness varies between 0.61 and 140 μm . The roughness for the bare and the sandblasted rods was measured by a profilometer. The grain size, or grit, which is a particle diameter of sandpaper, was provided by the sandpaper manufacturers. Grit was used to denote the size of roughness for rods half-covered with sandpaper. The height of the rods is 120 mm, much greater than the wavelength of sound and justifies two-dimensional approximation.

A phononic crystal used for experimental demonstration of the effects of asymmetry and non-reciprocity is shown in figure 2. Stainless steel rods of diameter $D=6.35\,\mathrm{mm}$ were cut from quarter-inch stock and arranged in a square lattice with period $a=10.30\,\mathrm{mm}$. Each rod was masked using a mould and a razor blade to uniformly cover half of the rod with tape. The tape acted as a resist when the rods were sandblasted to create lower levels of surface roughness. For increased roughness, a grit of sandpaper was chosen for testing with the thickness of the sandpaper measured as a tenth of a millimetre. The sandpaper covering precisely half of the cylindrical surface was cut using a laser cutter. After the sandpaper strips were cut to size, they

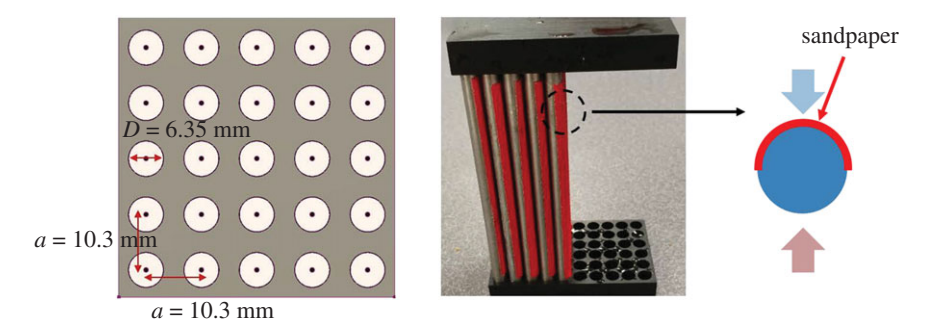


Figure 2. The cross-section view of the phononic crystals and 5×5 sample used in the experiment. The filling fraction $f \approx 0.3$. The cylinder scatterers are roughened on half their cylindrical surface through sandblasting or sandpaper of various grain sizes. (Online version in colour.)

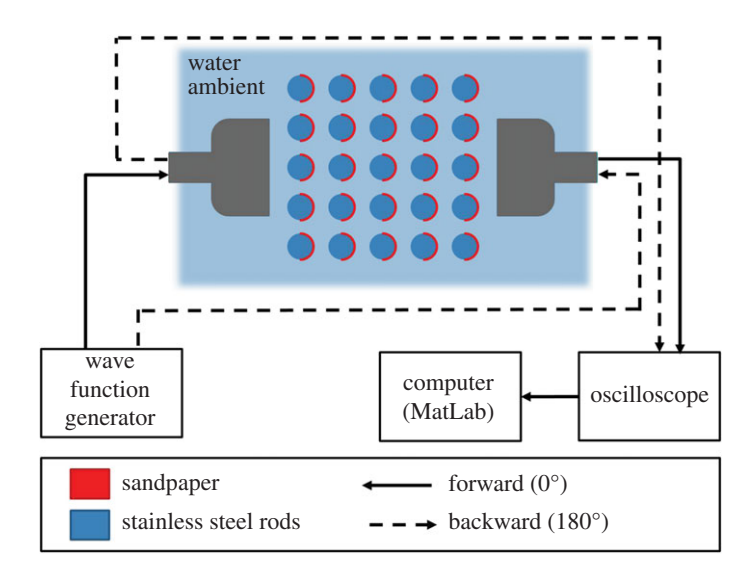


Figure 3. The schematic diagram of the experimental set-up of the ultrasound measurement. Transducers and phononic crystal are immersed in water. The phononic crystal is fixed by the support plate on the top and the bottom. For two opposite directions of wave propagation, the source and the receiver were interchanged. (Online version in colour.)

were glued to the rods using cyanoacrylate adhesive to have the best bond between the sandpaper and the steel rod. Once the desired number of rods had been manufactured (25 rods for each sample), they were fixed by top and bottom supports.

Spectra for the experiments were measured using a thru-transmission set-up. Two 1'' Panametrics V301 0.5 MHz immersion transducers were placed in a bi-static arrangement at opposing ends of the phononic crystal samples, each equidistant from the phononic crystal surface, see figure 3. The emitter was connected to a Wavestation 2012 Function Generator set to 20 Vpp, sweeping from 400 to 600 kHz over a 300 s timespan. Detection was accomplished with the receiving transducer connected to a Tektronix MDO 3024b Spectrum Analyzer set to 600 Hz resolution bandwidth. The entire set-up was in deionized ambient water. Data were acquired by sweeping the emitter within the range 400–600 kHz, recording the transmission, clearing the spectra, then reversing the leads of the emitter and detector and repeating the process. Multiple measurements were recorded to obtain a statistical average. The direction of the incident wave illuminating the smooth side of the rods is marked as 0° . The opposite direction of propagation is 180° . Along these directions P symmetry is broken. The perpendicular directions labelled by 90° and 270° are P-symmetric, i.e. statistically indistinguishable.

Reflection of an incident wave from the statistically rough surface leads to partial scattering in the directions different from specular. Phenomenologically the probability of specular reflection can be described by the specularity parameter ρ_F introduced by Fuchs [34]. Accordingly, the probability of non-specular (diffuse) reflection is $1 - \rho_F$. For a sufficiently smooth rough surface, the expansion of $1 - \rho_F$ over the height of roughness σ starts from the quadratic term,

$$1 - \rho_F \sim (\sigma k_t)^2 \sim \left(\frac{\sigma}{\lambda}\right)^2, \quad k_t \sigma \ll 1, \tag{2.1}$$

where k_t is the tangential to the surface projection of the wavevector and $\lambda = 2\pi/k$. Equation (2.1) is a result of the first Born approximation for weak scattering potential associated with roughness, e.g. [35].

For frequencies within the interval 400–600 kHz, the wavelength λ changes from 3.7 to 2.5 mm. For any frequency from this region, the inequality $\sigma \ll \lambda$ is satisfied, even for the roughness with $\sigma = 140~\mu\text{m}$, and justifies application of equation (2.1). At the same time, it is important to note that the theory of scattering at rough surfaces was developed for ideal inviscid fluids. The presence of a viscous boundary layer $\delta = \sqrt{2\eta/\rho\omega}$ may strongly modify the diffuse component of scattered field. If the roughness is completely covered by a viscous layer, $\sigma < \delta$, the weak diffuse component is suppressed since viscous dissipation is enhanced near any imperfection of a flat surface, especially near sharp corners. This means that reflection in a viscous fluid is more specular than reflection from the same rough surface in an ideal fluid. It is expected that dissipation makes the landscape of a rough surface smoother, thus reducing the diffuse component stronger than the specular one. A noticeable diffuse scattering appears for roughness exceeding the width of the viscous layer, $\sigma > \delta$.

Evolution of the measured transmission spectrum with gradual increase of surface roughness is shown in figure 4. The transmission coefficient *T* is defined as the ratio of sound intensities

$$T = \frac{I_{\text{rec}}}{I_{\text{emit}}}. (2.2)$$

The thickness of the viscous layer for the frequencies $\sim 0.5\,\mathrm{MHz}$ is about $1\,\mu\mathrm{m}$. Therefore, the spectra obtained for roughness $\sigma = 0.68\,\mu\mathrm{m}$ in figure 4a are practically reciprocal. The difference in transmission $T_{0^\circ} - T_{180^\circ}$ does not exceed the precision of the measurement. All other transmission spectra in figure 4 were obtained for the samples with roughness that exceeded δ by at least an order of magnitude. Due to asymmetric diffuse scattering at the rough cylindrical surfaces, the scatterers are non-reciprocal along the direction with broken P symmetry ($0^\circ \leftrightarrow 180^\circ$). At the same time, all the spectra measured along the P-symmetric direction ($90^\circ \leftrightarrow 270^\circ$) are reciprocal, independent of the size of roughness. The measure of non-reciprocity $T_{0^\circ} - T_{180^\circ}$ does not remain constant but changes and even alternates its sign with frequency. This occurs because the asymmetric and diffuse components of transmission results from multiple scattering events and interference (constructive or destructive) among them.

The overall transmission decreases essentially with size of roughness. This occurs not only due to higher viscous losses but also due to lateral radiative losses, which grow with diffusivity of the cylindrical surfaces. There is one more important factor—absorption by a narrow paper layer. This can be seen from the transmission spectra in figure 4b,c. While the roughness increases from 1.36 to $9.2\,\mu\text{m}$, this factor by itself cannot lead to two orders of magnitude decrease in transmission. Numerically simulated spectra with the same sizes of roughness but without the layer of sandpaper give only an approximately 15% decrease of overall transmission. Strong dissipative losses not only decrease the transmission but also lead to smoothen band-gap edges and general red shift of the spectra.

Two reasons cause the observed non-reciprocity: asymmetry in transmission, which is not related to viscosity and exists even in inviscid background, and different absorption originated from asymmetric distribution of velocities. The former reason is of a geometrical nature and the latter is related to broken *PT* symmetry that gives rise to truly non-reciprocal transmission. It

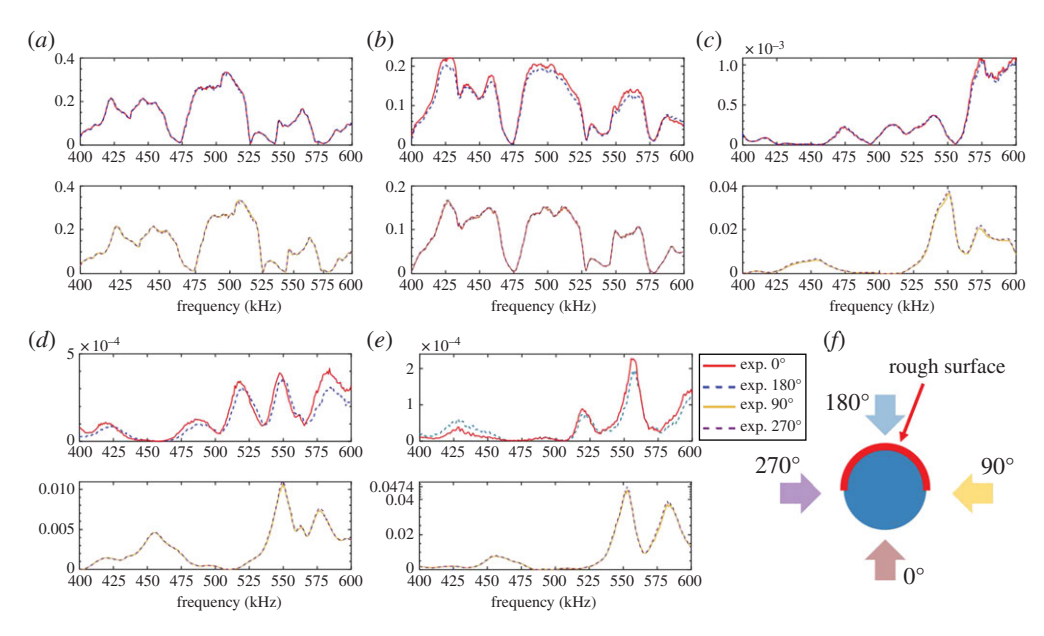


Figure 4. Experimental transmission spectra obtained for phononic crystals of rods with different roughness. (a) The stainless steel rods with natural roughness $\sigma = 0.61 \,\mu\text{m}$. (b) The half-sandblasted rods with $\sigma = 1.36 \,\mu\text{m}$. (c-e) The rods half-covered with the sandpaper with roughness $\sigma = 9.2 \,\mu\text{m}$ (c), 68 $\,\mu\text{m}$ (d) and 140 $\,\mu\text{m}$ (e), respectively. (f) The directions of the incident wave are shown with respect to the orientation of asymmetric scatterer. (Online version in colour.)

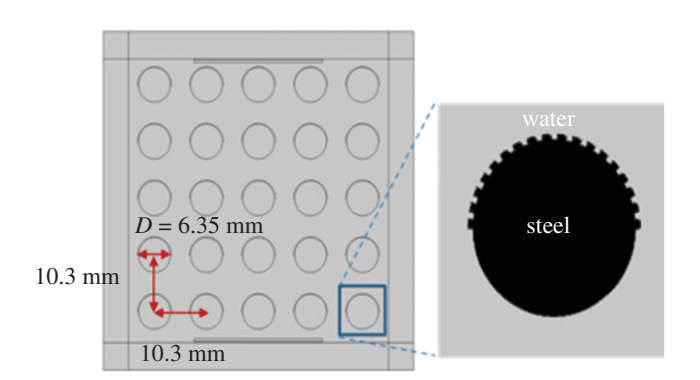


Figure 5. The cross-section view of phononic crystals with the parameters for the numerical simulation. To mimic roughness, rectangular tips are uniformly distributed along half the surface of the cylinders. The height of tips is a function of the desired size of roughness. The simulation boundaries are perfectly matched layers to absorb scattered waves that escape the simulation area (PML). (Online version in colour.)

is not possible to separate these two contributions in the experiment. We proceed to numerical simulation in order to extract the dissipative contribution responsible for the non-reciprocal part.

3. Numerical simulations of sound transmission

The transmission coefficient and dissipated energy are calculated using numerical (COMSOL) solutions of the linearized Navier–Stokes equation for a 5×5 phononic crystal. All the parameters were taken the same as in the experiment. Figure 5 illustrates the design of the phononic crystal. The insert shows the microstructure to mimic roughness. A rough surface is represented by a

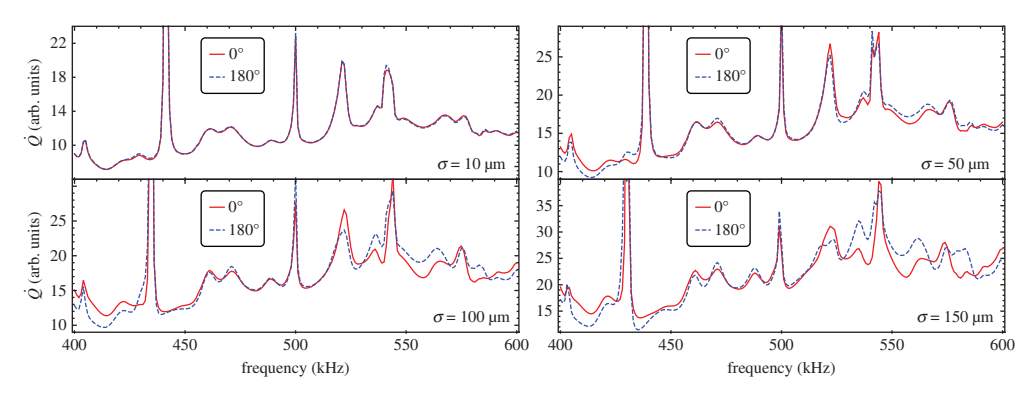


Figure 6. Numerically calculated spectra of dissipated energy for the direction of weakly broken *P* symmetry. Reciprocal spectra for propagation along the symmetric direction are not shown. (Online version in colour.)

rectangular relief with evenly distributed indents and barriers. The number of periods along the half-circle is 18 and it remains the same for different values of σ . While the regular relief is different from a statistically rough surface, it does not generate a strong regular pattern for a scattered field because the grating is not flat but lies on a cylindrical surface. Also, the wavelength of the propagating Bloch wave is much larger than σ , thus excluding noticeable diffraction effects. The largest mesh element size was smaller than one tenth of the smallest roughness size and the boundary layer was modelled to consider viscous effect for all the interfaces between solid and fluid. The phononic crystal is surrounded by perfectly matched layer.

The transmission coefficient defined as

$$T = \frac{\int_{rec} p(\mathbf{r}) v_x(\mathbf{r}) d\mathbf{r}}{\int_{omit} p(\mathbf{r}) v_x(\mathbf{r}) d\mathbf{r}}$$
(3.1)

exhibits non-reciprocity qualitatively similar to that observed in the experiment. Here, v_x is the projection of velocity to the direction from the emitter to receiver and integration runs over their areas.

Viscous losses of a signal transmitted from the emitter to receiver can be calculated as [13]

$$\dot{Q} = -\int \left[\frac{\eta}{2} \left(\frac{\partial v_i}{\partial x_k} + \frac{\partial v_k}{\partial x_i} - \frac{2}{3} \delta_{ik} \frac{\partial v_l}{\partial x_l} \right)^2 + \xi \left(\nabla \cdot \mathbf{v} \right)^2 \right] dV, \tag{3.2}$$

where integration runs over the volume of the sample. For two-dimensional phononic crystal of infinite rods the integral is taken over the cross section shown in figure 5. The viscosity coefficients η and ξ are sufficiently small in free water, where viscous losses are usually neglected. However, due to formation of a narrow viscous boundary layer around each solid scatterer the viscous losses are drastically enhanced, leading to 2–3 orders of magnitude higher losses than in free water [36].

Spectra of dissipated energy calculated for different roughness are presented in figure 6. The non-reciprocity is clearly seen and it becomes more pronounced for stronger roughness and higher frequencies. Dissipated energy is proportional to the length of the viscous layer, i.e. to the length of solid-fluid boundary. Since the number of periods on the rough part remains the same (18 periods), the length of the rough boundary increases by $2 \times 18 \cdot \sigma$ when compared with the length of flat boundary. Even for the largest roughness $\sigma = 150\,\mu\text{m}$ this increase is only 4 mm, much less than the circumference $\pi D \approx 20\,\text{mm}$. Neglecting the factor of length increase, we conclude that the non-reciprocity in dissipation is due solely to diffuse scattering, and it scales with σ as

$$\dot{Q}_{0^{\circ}} - \dot{Q}_{180^{\circ}} \sim (1 - \rho_F) \sim (k\sigma)^2.$$
 (3.3)

For the case of randomly rough surface the left-hand side of equation (3.3) is averaged over statistical ensemble of rough surfaces. Here, the averaging over statistical ensemble is replaced

by averaging over a narrow frequency interval 457–461 kHz. Within this interval the wavelength of propagating wave changes by $\Delta\lambda\approx30\,\mu\text{m}$. Since $\Delta\lambda$ makes up a considerable part of size of surface roughness, each wave 'illuminating' the rough surface generates essentially different diffuse field, while scattering at the cylinder as a whole remains unchanged. Thus, for the waves within the frequency interval 457–461 kHz the same rough surface 'looks' like different representatives from the same statistical ensemble, i.e. a kind of statistical averaging is realized.

Within the selected interval of frequencies the effects of the band structure that cause change of the sign of $\dot{Q}_{0^{\circ}}-\dot{Q}_{180^{\circ}}$ are sufficiently weak. In figure 7, the points obtained for $\sigma=50$, 100 and 150 μ m were fitted by a power law. The exponent of the power law is 2.1 that confirms the diffuse origin of non-reciprocity in dissipation. It follows from figure 6 that for the surface with roughness 150 μ m the selected interval of frequencies does not provide sufficiently wide variety of representatives of statistical ensemble. Because of this lack of averaging the point corresponding to the roughness 150 μ m lies slightly higher, which leads to the value of exponent 2.1 instead of 2.

The non-reciprocity in dissipation contributes to the non-reciprocity in transmission. This part is truly non-reciprocal since it leads to different decay of the transmitted signal. It was mentioned in [22] that '...there is no counter-example whereby an introduction of linear dissipation would destroy reciprocity, unless dissipation changes when the wave propagation direction is reversed...'. The presented results based on numerical solution of Navier–Stokes equation clearly demonstrate that in a system with broken P symmetry, dissipation turns out to be different for the opposite directions of propagation.

Non-reciprocity in dissipation in figure 6 is small because P symmetry is weakly broken by subwavelength roughness. Strong P symmetry breaking induces much stronger non-reciprocity in transmission [26]. Also, specially selected profile of roughness gives rise to much stronger absorption [33], however, for such profile σ^2 scaling for the probability of diffuse scattering is not valid.

This section demonstrates the effect of non-reciprocity in transmission through a finite-size sample with broken *PT* symmetry. In what follows we demonstrate how broken *PT* symmetry is manifested in scattering at a single rigid rod.

4. Scattering at a single asymmetric rod

Subwavelength surface roughness convert an isotropic cylinder to a slightly asymmetric scatterer. In figure 8, a polar diagram represents far-field distribution of square of pressure around a rigid cylinder without roughness (red and blue lines) and around a cylinder with $\sigma=10\,\mu\text{m}$ (green) and $\sigma=100\,\mu\text{m}$ (grey). The surrounding medium is inviscid water. The incoming plane wave is coming from the left, which corresponds to 0° direction. It illuminates the rough part of the cylindrical surface. The diameter of the cylinder is the same as was used in the experiment, $D=6.35\,\text{mm}$, and the frequency of the incoming wave is $508\,\text{kHz}$, which corresponds to the wavelength $\lambda=2.9\,\text{mm}$ in water. This frequency lies approximately in the centre of the used range of frequencies. The cylinder is a hard scatterer, i.e. its surface does not vibrate. Since the wavelength is less than half the diameter, the forward scattering dominates. The distribution of pressure for the smooth cylinder and for the cylinder with $10\,\mu\text{m}$ roughness is practically the same. For $100\,\mu\text{m}$ roughness, the peak in the forward direction is slightly extended. This is the only noticeable difference that does not change the scattering pattern. This graph demonstrates that the introduced roughness has a negligible effect on scattering.

In the next step, the validity of the reciprocal relation equation (1.1) has been verified. This requires a point-like source and receiver. A circular source domain of diameter 1 μ m is displaced at point A(B) at a distance r = 5 mm from the centre. The receiver of the same size is symmetrically displaced at point B(A), as shown in figure 9. The source generates a cylindrical wave with frequency 565 kHz ($\lambda = 2.6$ mm). For this frequency, the emitter and receiver can be safely considered as point objects.

The non-reciprocity of pressure can be characterized by the ratio

$$\Delta_p = 2 \frac{p_A(B) - p_B(A)}{p_A(B) + p_B(A)'} \tag{4.1}$$

calculated for fixed positions A and B. It was calculated for gradually increasing normalized viscosity of the environment, η/η_{water} . The numerical values for Δ_p presented in figure 9 are very small and they do not grow with viscosity. This result suggests that pressure is a reciprocal quantity even in a viscous fluid.

Oscillating velocity in a viscous fluid can be represented as a superposition of acoustic and vorticity modes, e.g. [37]

$$\mathbf{v}(\mathbf{r}) = \mathbf{v}_{ac} + \mathbf{v}_{vor},\tag{4.2}$$

where $\mathbf{v}_{ac}(\mathbf{r})$ is a potential and $\mathbf{v}_{vor}(\mathbf{r})$ is a solenoidal field. The acoustic mode is related to pressure $i\omega\rho\mathbf{v}_{ac}=\nabla p$ and in the principal approximation it is independent of viscosity. It can be calculated by the distribution of pressure in an ideal fluid. While the reciprocity relation (1.1) is valid for pressure, it is not valid for the gradient of pressure, provided broken P symmetry. This leads to non-reciprocity of the acoustic mode and finally to asymmetry in transmission. True non-reciprocity in transmission is due to the vorticity mode. It decays within the boundary layer δ , therefore this mode is sensitive to the shape of solid-fluid boundary. Coupling between the acoustic and vorticity modes occurs at the boundary and eventually leads to dissipative decay of sound.

Non-reciprocity for velocity fields was calculated for the positions of emitter and receiver at the same points A and B in figure 9 and the same frequency 565 kHz. The non-reciprocity is characterized by the quantity, Δ_v given by equation (4.1), where pressure is replaced by the modulus of velocity, $p \rightarrow v$. In figure 10 the non-reciprocity Δ_v is plotted versus normalized viscosity for the same roughnesses as in figure 9.

The graphs in figure 10 clearly demonstrate that the non-reciprocity in v, which exists even for the acoustic mode in ideal fluid $\eta=0$, grows fast with η . The difference $\Delta_v(\eta)-\Delta_v(\eta=0)$ is the contribution of the vorticity mode to non-reciprocity. Two curves for $\sigma=10$ and $100\,\mu\mathrm{m}$ demonstrate the same monotonic behaviour. Both curves exhibit square-root dependence at $\eta\to 0$. This behaviour is due to the Konstantinov effect of strong increase of viscous losses at reflection of sound from a solid-fluid boundary [38]. It is known that viscous losses at reflection grow $\sim \sqrt{\eta}$, unlike linear dependence for free viscous fluid. Since the pressure is reciprocal, the non-reciprocity in intensity and dissipation is proportional solely to non-reciprocity in velocity. Thus, the non-reciprocity in velocity scales as non-reciprocity in dissipation, i.e. $\Delta_v(\eta) - \Delta_v(\eta=0) \sim \sqrt{\eta}$. This scaling is valid for small values of η when the thickness of the viscous layer is much less than the wavelength. For the values of normalized viscosity used in figure 10 this condition is satisfied. For sound with frequency 565 kHz it is violated for $\eta/\eta_{\mathrm{water}} > 10^3$. Note that similar scaling with the coefficient that defines the anti-Hermitian part of the Hamiltonian was demonstrated for a response function of quantum non-Hermitian non-reciprocal system [39].

The values of non-reciprocity obtained for $\sigma=10\,\mu m$ (right vertical axis in figure 10) are approximately 10 times less than the values obtained for $\sigma=100\,\mu m$ (left vertical axis), i.e. $\Delta_{\nu}\sim\sigma$. This linear scaling of velocity corresponds to quadratic scaling of dissipation in figure 7 because according to equation (3.2) \dot{Q} is a quadratic functional of ${\bf v}$.

The asymmetry in transmission (and reflection) through a system of scatterers with broken P symmetry is related to non-reciprocity in the acoustic mode, which is practically independent of η and it does not vanish at $\eta=0$. Truly non-reciprocal contribution to transmission originates from the vorticity mode that defines the level of dissipation and the decay rate of sound in phononic crystal. An alternative opinion is expressed in [24] where it is stated that velocity by itself cannot serve as a criterion of reciprocity/non-reciprocity since only a product of dual variables (velocity × force = power) is invariant. Here we claim that this criterion may be linked to the velocity of the vorticity mode \mathbf{v}_{vor} , namely, to the quantity $\Delta_v(\eta) - \Delta_v(\eta=0)$, where the part due to asymmetry at $\eta=0$ is excluded.

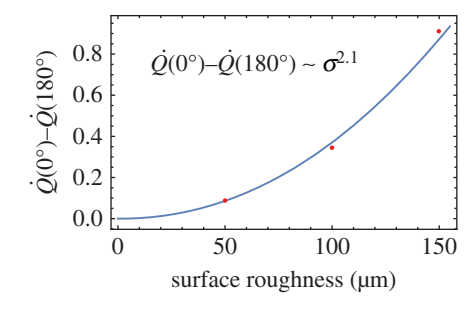


Figure 7. Red dots are the non-reciprocal part of dissipation averaged over range 457–461 kHz calculated for three values of surface roughness. The blue curve is a power law fitting $\sim \sigma^{2.1}$. (Online version in colour.)

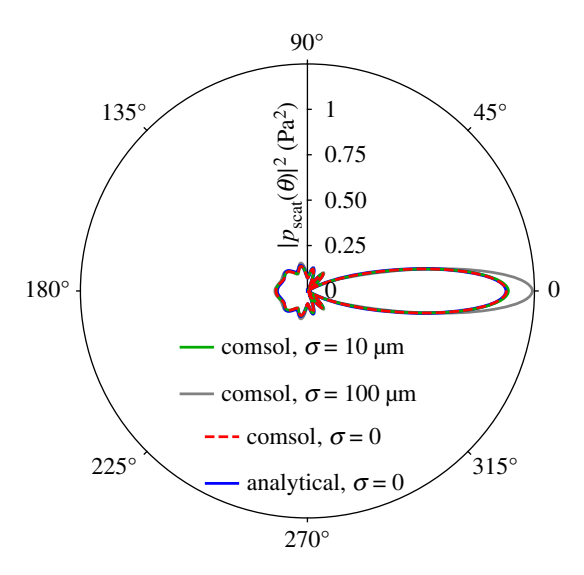


Figure 8. Polar distribution of $|p_{\text{scat}}(\theta)|^2$ around a rigid cylinder with smooth surface and cylinders with half-covered rough surface with $\sigma=10~\mu\text{m}$ and $\sigma=100~\mu\text{m}$. To control the accuracy of numerical calculations the result for smooth cylinder is obtained from known analytical expansion over Bessel functions and from numerical calculations. No difference is registered. (Online version in colour.)

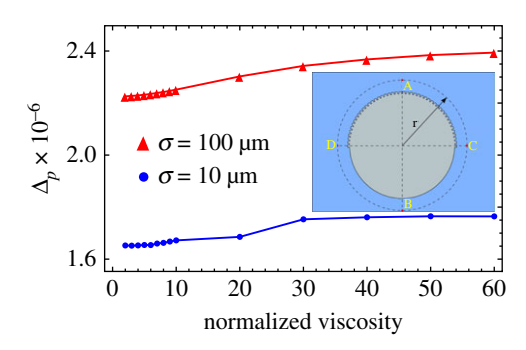


Figure 9. Non-reciprocity for pressure versus normalized viscosity η/η_{water} calculated for the source and receiver placed at the symmetrical points A and B situated 5 mm away from the centre. (Online version in colour.)

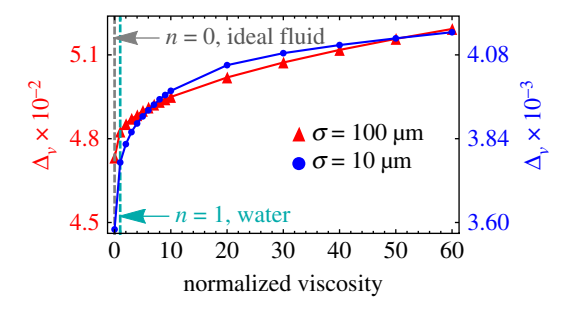


Figure 10. Non-reciprocity for velocity v versus normalized viscosity η/η_{water} calculated for the source and receiver placed at the symmetrical points A and B situated 5 mm away from the centre. The left (right) vertical axis is for roughness with $\sigma = 100 \, \mu\text{m}$ ($\sigma = 10 \, \mu\text{m}$). (Online version in colour.)

5. Acoustic reciprocity of an infinite phononic crystal

The question about non-reciprocity for an infinite system requires a criteria different from equation (1.1) since in a dissipative medium an emitter and a receiver separated by infinite distance do not communicate. In this sense, an infinite medium is *a priori* reciprocal because $p_A(B) = p_B(A) = 0$. Also, the criteria based on transmission is not applicable. Here, the reciprocity/non-reciprocity property of a medium can be considered from the point of view of the dispersion relation, namely, whether the equality $\omega(\mathbf{k}) = \omega(-\mathbf{k})$ is true or not.

The wave equation for velocity $\mathbf{v}(\mathbf{r},t)$ in an inhomogeneous fluid is obtained from the Navier–Stokes equation and continuity equation and reads [37]

$$\rho \ddot{v}_{i} - \frac{\partial}{\partial x_{i}} (\lambda \nabla \cdot \mathbf{v}) = \frac{\partial}{\partial x_{i}} (\xi \nabla \cdot \dot{\mathbf{v}}) + \frac{\partial}{\partial x_{k}} \left[\eta \left(\frac{\partial \dot{v}_{i}}{\partial x_{k}} + \frac{\partial \dot{v}_{k}}{\partial x_{i}} - \frac{2}{3} \delta_{ik} \nabla \cdot \dot{\mathbf{v}} \right) \right], \tag{5.1}$$

where λ is the elastic bulk modulus and ξ and η are the bulk and shear viscosity, respectively. In a phononic crystal, all the parameters ρ , λ , η and ξ are periodic functions represented by their Fourier series. Applying the Bloch theorem, the unknown function $\mathbf{v}(\mathbf{r},t)$ can be written in the form

$$\mathbf{v}(\mathbf{r},t) = e^{i(\mathbf{k}\cdot\mathbf{r} - \omega t)} \sum_{\mathbf{G}} \mathbf{v}(\mathbf{G})_{\mathbf{k}} e^{i\mathbf{G}\cdot\mathbf{r}}.$$
 (5.2)

Here, **G** is an infinite set of the reciprocal-lattice vectors.

Substituting the Bloch representation (5.2) into the wave equation (5.1) and using Fourier representation for all periodic functions, the following infinite set of linear equations for the components $\mathbf{v}(\mathbf{G})$ is obtained

$$\sum_{\mathbf{G}'} \left[\omega^{2}(\mathbf{k}) \rho(\mathbf{G} - \mathbf{G}') + i\omega(\mathbf{k})(\mathbf{k} + \mathbf{G}) \cdot (\mathbf{k} + \mathbf{G}') \eta(\mathbf{G} - \mathbf{G}') \right] \mathbf{v}_{\mathbf{k}}(\mathbf{G}') - (\mathbf{k} + \mathbf{G}) \sum_{\mathbf{G}'} \left\{ \lambda(\mathbf{G} - \mathbf{G}') - i\omega(\mathbf{k}) \left[\xi(\mathbf{G} - \mathbf{G}') - \frac{2}{3} \eta(\mathbf{G} - \mathbf{G}') \right] \right\} (\mathbf{k} + \mathbf{G}') \cdot \mathbf{v}_{\mathbf{k}}(\mathbf{G}')$$

$$= -i\omega(\mathbf{k}) \sum_{\mathbf{G}'} \eta(\mathbf{G} - \mathbf{G}')(\mathbf{k} + \mathbf{G}')(\mathbf{k} + \mathbf{G}) \cdot \mathbf{v}_{\mathbf{k}}(\mathbf{G}'). \tag{5.3}$$

Here, the Fourier components are defined as

$$\rho(\mathbf{G}) = \frac{1}{A_c} \int_{c} \rho(\mathbf{r}) e^{-i\mathbf{G} \cdot \mathbf{r}} d\mathbf{r}.$$
 (5.4)

Integration runs over the area of the unit cell A_c . The same definition is applied to all other periodic functions. If the inclusions are symmetric the Fourier components are real, otherwise $\rho(-\mathbf{G}) = \rho^*(\mathbf{G})$.

The set of equations (5.3) is not a standard eigenvalue problem since the dispersion relation $\omega(\mathbf{k})$ enters linearly and quadratically. An effective method of numerical solution of this type of equations was proposed in [40]. If the media are dissipationless, $\eta = \xi = 0$, equation (5.3) is reduced to a generalized eigenvalue problem. The eigenvalue $\omega^2(\mathbf{k})$ is real due to hermiticity of the kernels $\rho(\mathbf{G} - \mathbf{G}')$ and $\lambda(\mathbf{G} - \mathbf{G}')$. In a viscous phononic crystal the anti-Hermitian kernels (which are proportional to $\omega(\mathbf{k})$) give rise to an imaginary part of frequency. The dispersion relation is obtained by equating the determinant of the homogeneous set of equations (5.3) to zero.

Inversion of the Bloch vector \mathbf{k} in equation (5.3) and replacement $\mathbf{G} \to -\mathbf{G}$, $\mathbf{G}' \to -\mathbf{G}'$ leads to the set of equations where $\rho(\mathbf{G} - \mathbf{G}') \to \rho(\mathbf{G}' - \mathbf{G})$ with the same replacement for all other Fourier components

$$\sum_{\mathbf{G}'} \left[\omega^{2}(-\mathbf{k})\rho(\mathbf{G}' - \mathbf{G}) + i\omega(-\mathbf{k})(\mathbf{k} + \mathbf{G}) \cdot (\mathbf{k} + \mathbf{G}')\eta(\mathbf{G}' - \mathbf{G}) \right] \mathbf{v}_{-\mathbf{k}}(-\mathbf{G}') - (\mathbf{k} + \mathbf{G}) \sum_{\mathbf{G}'} \left\{ \lambda(\mathbf{G}' - \mathbf{G}) - i\omega(-\mathbf{k}) \left[\xi(\mathbf{G}' - \mathbf{G}) - \frac{2}{3}\eta(\mathbf{G}' - \mathbf{G}) \right] \right\} (\mathbf{k} + \mathbf{G}') \cdot \mathbf{v}_{-\mathbf{k}}(-\mathbf{G}')$$

$$= -i\omega(-\mathbf{k}) \sum_{\mathbf{G}'} \eta(\mathbf{G}' - \mathbf{G})(\mathbf{k} + \mathbf{G}')(\mathbf{k} + \mathbf{G}) \cdot \mathbf{v}_{-\mathbf{k}}(-\mathbf{G}'). \tag{5.5}$$

It is clear that if the inclusions are symmetric then the two sets of equations (5.3) and (5.5) are equivalent since all the Fourier components are even real functions of G - G'. However, even if the scatterers are asymmetric, the dispersion relation obtained from equations (5.3) and (5.5) are equal

$$\omega(\mathbf{k}) = \omega(-\mathbf{k}),\tag{5.6}$$

since they are obtained from the condition of vanishing the determinants of two mutually transpose matrices, $\det |a_{ik}| = \det |a_{ki}|$. This finalizes the proof of reciprocity of dispersion relation of phononic crystal with viscous constituents. Note that while this conclusion was obtained for a fluid-fluid phononic crystal, it remains true for any solid-fluid crystals as well. The only difference that appears in solid inclusion are the terms associated with the shear mode. However, the corresponding kernels also possess the same symmetry with respect to the replacement $(\mathbf{G} - \mathbf{G}') \to (\mathbf{G}' - \mathbf{G})$, therefore the reciprocity property equation (5.6) is valid for any combination of elastic materials in a phononic crystal.

The reciprocity for the Fourier components of velocity in an inviscid environment, which follows from equations (5.3) and (5.5) at $\eta = \xi = 0$, reads $\mathbf{v}_{-\mathbf{k}}^*(-\mathbf{G}) = \mathbf{v}_{\mathbf{k}}(\mathbf{G})$. This relation becomes invalid for a viscous phononic crystal since the linear over ω terms break the symmetry. Thus, even an infinite phononic crystal is not completely reciprocal because of the viscous friction terms in the right-hand side of equations (5.3) and (5.5) that break T symmetry of the wave equation.

Reciprocity is a well-known fundamental property of the eigenvalues of the Schrodinger equation in a periodic potential. Here, we give a direct proof that viscous losses introduced through the Navier–Stokes equation do not break this reciprocity, while the eigenfunctions become non-reciprocal.

A common phenomenological method to introduce dissipation in an elastic medium is to add an imaginary part to elastic constant [41]. This method is widely used to study the effects of viscous and viscoelastic damping on the dispersion relation in phononic crystals [42,43]. It follows from equation (5.3) that in a periodic viscous medium the elastic modulus and mass density become complex ω - and k- dependent matrices

$$\lambda(\mathbf{G}, \mathbf{G}') = \lambda(\mathbf{G} - \mathbf{G}') - i\omega(\mathbf{k}) \left[\xi(\mathbf{G} - \mathbf{G}') - \frac{2}{3}\eta(\mathbf{G} - \mathbf{G}') \right]$$
 (5.7)

and

$$\rho(\mathbf{G}, \mathbf{G}') = \left[\rho(\mathbf{G} - \mathbf{G}') + \frac{i}{\omega(\mathbf{k})} (\mathbf{k} + \mathbf{G}) \cdot (\mathbf{k} + \mathbf{G}') \eta(\mathbf{G} - \mathbf{G}') \right]. \tag{5.8}$$

Renormalization of the elastic modulus and mass density in a viscous fluid is predicted by a rather simple Rayleigh model [44]. Apart from these two terms, the microscopic approach based on the Navier–Stokes equation gives the term in the right-hand side of equation (5.3), which does not appear in the phenomenological model. This term takes into account the tensorial character of response of a viscous Newtonian fluid.

6. Conclusion

In conclusion, a non-reciprocal transmission of sound through a finite-length phononic crystal with asymmetric scatterers imbedded in a viscous environment have been demonstrated experimentally and numerically. Detailed calculations of dissipated acoustic energy have unambiguously revealed that the difference in energy transmitted through a phononic crystal in opposite directions contains two principally different contributions: a reciprocal one associated with asymmetry of the scatterers and a non-reciprocal one associated with dissipation. The carrier of the former is the acoustic mode—sound propagating in an inviscid fluid—and the carrier of the latter is the vorticity mode, which exists only in a viscous fluid where *T* symmetry is broken. The level of non-threciprocity and asymmetry in transmission can be controlled by measure of the broken *P* symmetry and the length of the sample. The non-reciprocity, which is due to the vorticity mode, vanishes for infinitely long samples. Accordingly, the transmission approaches zero for forward and backward directions of propagation. Viscosity-dependent non-reciprocity may find applications in the design of passive broadband devices for rectification of acoustic signals.

Prevailing literature surrounding reciprocity presents it as fundamentally a property of all elastic media, requiring broken T symmetry in nonlinear or moving media for non-reciprocity. Viscous losses, which break T symmetry, are not considered in acoustics as a nonreciprocal factor. Our prior experiments [25] proposed broken P symmetry as a passive mechanism to achieve non-reciprocity. In this work, we prove that in finite-length samples non-reciprocity is due to dissipative vorticity mode, which is usually missing, provided asymmetry is the necessary condition. For infinite dissipative phononic crystal, we prove that the decay coefficient is reciprocal but the velocity remains non-reciprocal due to broken PT symmetry.

For an infinite phononic crystal, broken *PT* symmetry does not affect the reciprocity of the eigenvalues, leaving the dispersion relation an even function of the Bloch vector. However, the reciprocity of the eigenfunctions is lost. In the case of electromagnetic waves dissipation is not considered as a factor leading to non-reciprocity, however, it may enhance the non-reciprocity in the presence of external magnetic field [45]. It was recently reported that a steady flow of viscous electron liquid considered in the hydrodynamic approximation exhibits strong non-reciprocity if *P* symmetry is broken [46]. This conclusion remains true for a flow of any classical fluid that satisfies Navier–Stokes equation. The origin of non-reciprocity in acoustics and hydrodynamics is the same: it is due to different dissipation (or resistance) in transmission (or flow) in forward and backward directions.

Data accessibility. This article does not contain any additional data.

Competing interests. We declare we have no competing interests.

Funding. This work was supported by the National Science Foundation under EFRI grant no. 1741677.

Acknowledgements. We are thankful to Michael Haberman for his initial suggestion regarding the shape of the scatterers.

References

- 1. Strutt (Rayleigh) JW. 1876 On the application of the principle of reciprocity to acoustics. *Proc. R. Soc.* **25**, 118. (doi:10.1098/rspl.1876.0025)
- 2. Schottky W. 1926 Das Gesetz des Tiefempfangs in der Akustik und Elektroakustik. *Z. Phys.* **36**, 689–736. (doi:10.1007/BF01400157)

- 3. Foldy LL, Primakoff N. 1945 A general theory of passive linear electroacoustic transducers and the electroacoustic reciprocity theorem. *J. Acoust. Soc. Am.* 17, 109; *ibid* 19, 50 (1947). (doi: 10.1121/1.1916305)
- 4. Laymshev LM. 1959 A question in connection with the principle of reciprocity in acoustics. *Sov. Phys. Doklady* **4**, 406.
- Chertock G. 1962 General reciprocity relation. J. Acoust. Soc. Am. 34, 989. (doi:10.1121/ 1.1918239)
- 6. De Hoop AT. 1966 An elastodynamic reciprocity theorem for linear, viscoelastic media. *Appl. Sci. Res.* **16**, 39–45. (doi:10.1007/BF00384053)
- 7. de Hoop AT. 1988 Time-domain reciprocity theorems for acoustic wave fields in fluids with relaxation. *J. Acoust. Soc. Am.* **84**, 1877. (doi:10.1121/1.397152)
- 8. Belousov Yu.I, Rimskii-Korsakov AV. 1974 The reciprocity principle in acoustics and its application to the calculation of sound field bodies. *Sov. Phys. Acoust.* 21, 103.
- 9. Godin OA. 1997 Reciprocity and energy theorems for waves in a compressible inhomogeneous moving fluid. *Wave Motion* 25, 143–167. (doi:10.1016/S0165-2125(96)00037-6)
- Allard JF. 1992 Propagation of sound in porous media. London and New York: Elsevier Applied Science.
- 11. Wapenaar K, Fokkema J. 2004 Reciprocity theorems for diffusion, flow, and waves. *J. Appl. Mech.* **71**, 145–150. (doi:10.1115/1.1636792)
- 12. Wapenaar K, Reinicke C. 2019 Unified wave field retrieval and imaging method for inhomogeneous non-reciprocal media. *J. Acoust. Soc. Am.* **146**, 810. (doi:10.1121/1.5114912)
- 13. Landau LD, Lifshitz EM. 1984 Fluid Mechanics, 2nd edn. Oxford, UK: Elsevier.
- 14. Krishnan R, Shirota S, Tanaka Y, Nishiguchi N. 2007 High-efficient acoustic wave rectifier. *Solid State Commun.* **144**, 194. (doi:10.1016/j.ssc.2007.08.036)
- 15. Shirota S, Krishnan R, Tanaka Y, Nishiguchi N. 2007 Rectifying acoustic waves. *Jpn J. Appl. Phys.* 46, L1025. (doi:10.1143/JJAP.46.L1025)
- 16. Liang B, Guo XS, Tu J, Zhang D, Cheng JC. 2010 An acoustic rectifier. *Nat. Mater.* **9**, 989–992. (doi:10.1038/nmat2881)
- 17. Li X-F, Ni X, Feng L, Lu M-H, He C, Chen Y-F. 2011 Tunable unidirectional sound propagation through a sonic-crystal-based acoustic diode. *Phys. Rev. Lett.* **106**, 084301. (doi:10.1103/PhysRevLett.106.084301)
- 18. He ZJ, Peng SS, Ye YT, Dai ZW, Qiu CY, Ke MZ, Liu ZY. 2011 Asymmetric acoustic gratings. *Appl. Phys. Lett.* **98**, 083505. (doi:10.1063/1.3562306)
- 19. Sun H, Zhang S, Shui X. 2012 Tunable acoustic diode made by a metal plate with periodical structure. *Appl. Phys. Lett.* **100**, 103507. (doi:10.1063/1.3693374)
- 20. Zangeneh-Nejad F, Fleury R. 2019 Acoustic rat-race coupler and its applications in non-reciprocal systems. *J. Acoust. Soc. Am.* **146**, 843. (doi:10.1121/1.5115020)
- 21. Zhu J, Zhu X, Yin X, Wang Y, Zhang X. 2020 Unidirectional extraordinary sound transmission with mode-selective resonant materials. *Phys. Rev. Appl.* **13**, 041001. (doi:10.1103/PhysRevApplied.13.041001)
- 22. Maznev AA, Every AG, Wright OB. 2013 Reciprocity in reflection and transmission: what is a 'phonon diode'? *Wave Motion* **50**, 776. (doi:10.1016/j.wavemoti.2013.02.006)
- 23. Fleury R, Sounas D, Haberman MR, Alù A. 2015 Nonreciprocal acoustics. Acoust. Today 11, 14.
- 24. Nassar H, Yousefzadeh B, Fleury R, Ruzzene M, Alú A, Daraio Ch., Norris AN, Huang G, Haberman MR. 2020 Nonreciprocity in acoustic and elastic materials. *Nat. Rev. Mater.* 5, 667–685. (doi:10.1038/s41578-020-0206-0)
- 25. Tanaka Y, Shimomura Y, Nishiguchi N. 2018 Acoustic wave rectification in viscoelastic materials. *Jpn. J. Appl. Phys.* 57, 034101. (doi:10.7567/JJAP.57.034101)
- 26. Walker E, Neogi A, Bozhko A, Zubov Yu., Arriaga J, Heo H, Ju J, Krokhin AA. 2018 Nonreciprocal linear transmission of sound in a viscous environment with broken P symmetry. *Phys. Rev. Lett.* **120**, 204501. (doi:10.1103/PhysRevLett.120.204501)
- 27. Pierce AD. 2018 Reciprocity theorems and perception of non-reciprocal behavior in vibrating systems, metamaterials, acoustic devices, and electroacoustic devices. *J. Acoust. Soc. Am.* **143**, 1946. (doi:10.1121/1.5036376)
- 28. Merkel A, Theocharis G, Richoux O, Romero-García V, Pagneux V. 2015 Control of acoustic absorption in one-dimensional scattering by resonant scatterers. *Appl. Phys. Lett.* **107**, 244102. (doi:10.1063/1.4938121)
- 29. Wei P, Croëenne C, Tak Chu S, Li J. 2014 Symmetrical and anti-symmetrical coherent perfect absorption for acoustic waves. *Appl. Phys. Lett.* **104**, 121902. (doi:10.1063/1.4869462)

- 30. Merkel A, Romero-García V, Groby J-P, Li J, Christensen J. 2018 Unidirectional zero sonic reflection in passive *PT*-symmetric Willis media. *Phys. Rev. B.* **98**, 201102. (doi:10.1103/PhysRevB.98.201102)
- 31. Norris AN, Packo P. 2019 Non-symmetric flexural wave scattering and one-way extreme absorption. *J. Acoust. Soc. Am.* **146**, 873. (doi:10.1121/1.5087133)
- 32. Wu Q, Chen Y, Huang G. 2019 Asymmetric scattering of flexural waves in a parity-time symmetric metamaterial beam. *J. Acost. Soc. Am.* **146**, 850–862. (doi:10.1121/1.5116561)
- 33. Lee H, Jung M, Kim M, Shin R, Kang S, Ohm W-S, Tae Kim Y. 2018 Acoustically sticky topographic metasurfaces for underwater sound absorption. *J. Acoust. Soc. Am.* **143**, 1534. (doi:10.1121/1.5027247)
- 34. Fuchs K. 1938 The conductivity of thin metallic films according to the electron theory of metals. *Math. Proc. Camb. Phil. Soc.* 34, 100–862. (doi:10.1017/S0305004100019952)
- 35. Bass FG, Fuks IM. 1979 Wave scattering from statistically rough surfaces. Oxford, UK: Pergamon Press.
- 36. Ibarias M, Zubov Yu., Arriaga J, Krokhin AA. 2020 Phononic crystal as a homogeneous viscous metamaterial. *Phys. Rev. Res.* **2**, 022053. (doi:10.1103/PhysRevResearch.2.022053)
- 37. Piers AD. 2019 *Acoustics, an introduction to its physical principles and applications,* 3rd edn. Cham: Springer.
- 38. Konstantinov BP. 1939 To the problem of sound absorption at reflection from a solid boundary. *Zh. Tekh. Fiz.* **9**, 226.
- 39. Lau H-K, Clerk AA. 2018 Fundamental limits and non-reciprocal approaches in non-Hermitian quantum sensing. *Nat. Commun.* **9**, 4320. (doi:10.1038/s41467-018-06477-7)
- 40. Hussein M. 2009 Reduced Bloch mode expansion for periodic media band structure calculations. *Proc. R. Soc. A* 465, 2825–2848. (doi:10.1098/rspa.2008.0471)
- 41. Tschoegl NW. 1989 The phenomenological theory of linear viscoelastic behavior. Heidelberg: Springer.
- 42. Hussein MI, Frazier MJ. 2013 Damped phononic crystals and acoustic metamaterials. In *Acoustic Metamaterials and Phononic Crystals* (ed. PA Deymier). Berlin, Heidelberg: Springer.
- 43. Frazier MJ, Hussein MI. 2015 Viscous-to-viscoelastic transition in phononic crystal and metamaterial band structures. *J. Acoust. Soc. Am.* **138**, 3169–3180. (doi:10.1121/1.4934845)
- 44. Rayleigh JWS. 1896 *The theory of sound*, 2nd edn., Ch. XIX § 345. New York, NY: Macmillan and Co.
- 45. Monticone F. 2020 A truly one-way lane for surface plasmon polaritons. *Nat. Photon.* **14**, 461–465. (doi:10.1038/s41566-020-0662-5)
- 46. Geurs J, Kim Y, Watanabe K, Taniguchi T, Moon P, Smet JH. Rectification by hydrodynamic flow in an encapsulated graphene Tesla valve. (http://arxiv.org/abs/2008.04862v1).